THE JOURNAL OF PHYSICAL CHEMISTRY B

Article

pubs.acs.org/JPCB

Molecular Motion of the Bis(maleonitriledithiolato)nickel Trianion in Solution

Bruce A. Kowert,*[,†] Ann B. J. Stemmler,[‡] Timothy L. Stemmler,[‡] Steven J. Gentemann,[§] Michael B. Watson,[∥] and Vanessa S. Goodwill [†]

[†]Department of Chemistry, St. Louis University, 3501 Laclede Ave., St. Louis, Missouri 63103, United States

[‡]Department of Biochemistry & Molecular Biology, Wayne State University, 540 E. Canfield Ave., Detroit, Michigan 48201, United States

[§]Southwestern Illinois College, 2500 Carlyle Ave., Belleville, Illinois 62221, United States

[∥]Department of Chemistry, Washington University, One Brookings Drive, St. Louis, Missouri 63130, United States

Supporting Information

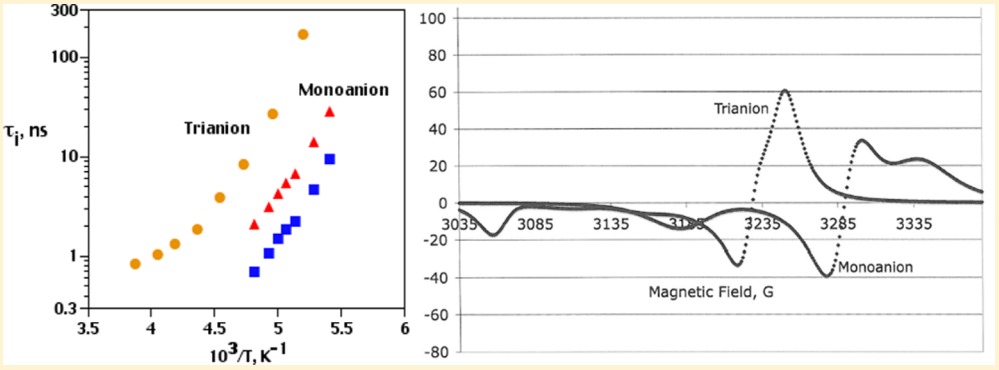

ABSTRACT: Electron spin resonance (ESR) has been used to study the reorientational motion of the bis(maleonitriledithiolato)nickel trianion, $[Ni(mnt)_2]^{3-}$, in diethylene glycol dimethyl ether (diglyme). $[Ni(mnt)_2]^{3-}$ has one unpaired electron and was prepared by reducing the dianion, $[Ni(mnt)_2]^{2-}$, with potassium metal. The trianion and dianion are members of the redox series $[Ni(mnt)_2]^{n-}$ with n = 0, 1, 2, and 3. The monoanion, $[Ni(mnt)_2]^{-}$, also has S = 1/2 and its rotational diffusion in diglyme was the subject of previous ESR studies. This made possible the comparison of the reorientational data for two different oxidation states of the same planar complex in the same solvent. Differences were found; isotropic rotational diffusion produced agreement between the trianion's experimental and calculated spectra, whereas the monoanion's simulations required axially symmetric reorientation with diffusion about the long in-plane axis three times faster than that about the two perpendicular axes. At a given temperature, the monoanion's reorientation rates about the long in-plane axis and two perpendicular axes were faster than the trianion's isotropic rate by factors of ~27 and ~9, respectively. These differences suggest that $[Ni(mnt)_2]^{-}$ and $[Ni(mnt)_2]^{3-}$ have different shapes and sizes in solution; the monoanion is approximately a prolate ellipsoid, whereas the trianion is larger and more spherical. $[Ni(mnt)_2]^{3-}$ appears to be ion-paired, whereas in accord with results from other techniques, $[Ni(mnt)_2]^{-}$ is not.

1. INTRODUCTION

Metallo-bis(dithiolene) complexes, $[M(mnt)_2]^{n-}$, have received considerable attention because of their multiple oxidation states.[1,2] Nickel complexes (Figure 1) with n = 0, 1, 2, and 3 have been prepared.[2−7] The anions with n = 1 and 3 are paramagnetic (S = 1/2) and have been studied by several different magnetic resonance methods.

Maki and co-workers[8] used single-crystal ESR to assign the g factors of planar $[Ni(mnt)_2]^{-}$ to the symmetry axes in Figure 1. Another single-crystal ESR experiment[9] provided the monoanion's ^{33}S hyperfine tensor while the ^{61}Ni hyperfine principal values were obtained from the glassy spectrum of an isotopically enriched sample.[8] The spin densities at mnt's

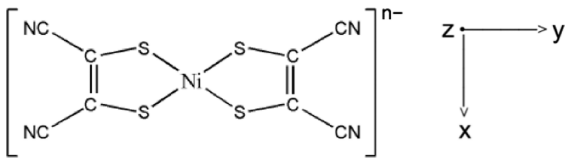

Figure 1. Molecular structure of $[Ni(mnt)_2]^{n-}$ and the right-handed principal axes of the anisotropic Zeeman interaction.

Received: March 18, 2012
Revised: June 8, 2012
Published: June 25, 2012

 © 2012 American Chemical Society

carbons and nitrogen were determined[10] using ENDOR and ESEEM spectroscopies.

The chemical and physical dynamics of the monoanion also have been studied. Carbon-13 NMR was used to determine k_{ex}, the rate constant for the self-exchange (electron transfer) reaction between $[Ni(mnt)_2]^-$ and the dianion, $[Ni(mnt)_2]^{2-}$; the values of k_{ex} in acetone and nitromethane were faster than those for other Ni(III,II) couples but in general agreement with the predictions of Marcus theory.[11]

Analyses of the monoanion's solution ESR spectra[12−18] showed the rotational diffusion about its long in-plane (y) axis to be 3−4 times faster than that about the two perpendicular (x, z) axes; this indicated, along with results from other techniques (discussed below), that the shape of the paramagnetic solute was comparable to that of free $[Ni(mnt)_2]^-$. The solvents were *n*-butyl alcohol (BuOH), ethyl alcohol (EtOH), 4-allyl-2-methoxyphenol (eugenol), dimethyl phthalate (DMPT), tri-*n*-butyl phosphate (TBP), tris(2-ethyl-hexyl)-phosphate (TEHP), a dimethylformamide-chloroform mixed solvent (DMF-$CHCl_3$), and four ethers, including diethylene glycol dimethyl ether (diglyme).

The air-sensitive trianion, $[Ni(mnt)_2]^{3-}$, was first prepared using vacuum electrochemical techniques[2,6,7] and has not been studied to the same extent. Geiger et al.[6,7] obtained the trianion's ^{61}Ni hyperfine principal values and g factors from glassy spectra with and without ^{61}Ni-enrichment, respectively; the spectra were taken in dimethoxyethane (DME) as was a motionally narrowed spectrum. No spectra were reported between the two limits.

We were interested in studying the solution dynamics of $[Ni(mnt)_2]^{3-}$ via ESR but did not have vacuum electrochemical capabilities. DME, however, has long been a solvent in which aromatic radical anions have been prepared by alkali metal reduction.[19] Diglyme, like DME, is a polyether and $[Ni(mnt)_2]^{2-}$ could be reduced to $[Ni(mnt)_2]^{3-}$ in both using potassium metal. It was not possible to obtain spectra over the entire range of motional averaging in DME because it does not become sufficiently viscous before freezing. Diglyme, however, has a wider range of viscosities and spectra could be taken in the intermediate and slow motional regions, as they were for the monoanion. This allowed us to simulate the trianion's spectra and compare the temperature-dependent reorientational data of two different oxidation states of the same complex in the same solvent. Because of its more negative charge, the motional characteristics of the trianion might be expected to be different from those of the monoanion. In fact, $[Ni(mnt)_2]^{3-}$ was found to be reorienting more slowly than $[Ni(mnt)_2]^-$ via isotropic, not axially symmetric, diffusion; these differences are discussed in terms of the two ions' interactions with solution components.

2. EXPERIMENTAL SECTION

2.1. Chemicals and Purification. As described in ref 17, diglyme (Fisher Scientific Co., bp 162 °C) was purified using multiple distillations from potassium metal and lithium aluminum hydride (LAH) and then stored on a vacuum line over LAH; the same procedure was used for DME (Eastman Chemical Co, bp 85 °C).

2.2. Trianion Preparation. The method used to reduce the dianion in diglyme and DME is outlined here; additional details and a description of the sample cell are given in the Supporting Information. The tetrabutylammonium salt of the dianion, $(Bu_4N)_2[Ni(mnt)_2]$,[20] was placed in the sample cell on a vacuum line, purified solvent was distilled into the cell, and the cell was sealed off. The dianion solution was brought over a potassium mirror while cooling the sample cell with glass wool dipped in an acetone−dry ice bath. The resulting trianion solution was poured into a 3 mm o.d. Pyrex tube attached to the cell, which was transferred directly to the precooled cavity of an X-band ESR spectrometer. The $[Ni(mnt)_2]^{3-}$ concentration was ~10^{-3} M.

The glassy spectrum of $[Ni(mnt)_2]^{3-}$ in diglyme was recorded at −98.0 °C (Figure 2) after which the temperature

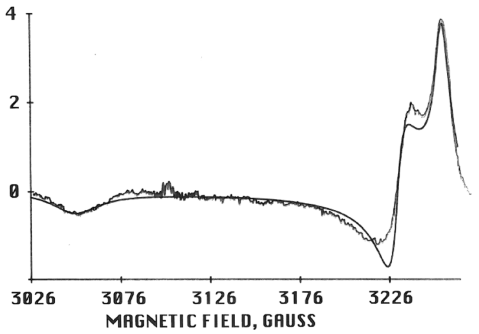

Figure 2. Glassy spectrum of $[Ni(mnt)_2]^{3-}$ in diglyme at −98.0 °C and a spectrum calculated using g_x = 2.0824, g_y = 2.0660, and g_z = 2.2053.

was raised and motionally averaged spectra were taken between −81.0 and −15.5 °C; those for −53.0, −62.0, and −71.5 °C are compared with calculated spectra in Figures 3−7. Spectra for all

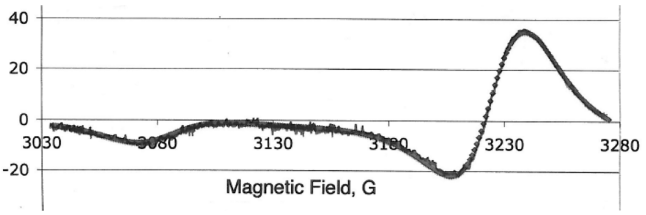

Figure 3. Motionally averaged spectrum of $[Ni(mnt)_2]^{3-}$ in diglyme at −53.0 °C and a spectrum calculated using the glassy g_i, isotropic BRD, $D_\perp = 4.4 \times 10^7$ s^{-1}, and $T_2^{-1} = 0.150F_0$ (7.4−8.4 G).

temperatures are included in the Supporting Information; they show an additional signal upfield from the trianion's that has been assigned to the solvated electron. It has a g value (2.0022) consistent with those found using potassium metal in tetrahydrofuran[21] (2.0019) and the crown ethers[22] 15-crown-5 (2.0027) and 12-crown-4 (2.0020). The singlet was not seen in the trianion spectra in DME or in any of the $[Ni(mnt)_2]^-$ spectra, which spanned magnetic fields ranging from $1.9951 \leq g \leq 2.1440$.[15−17] All of our $[Ni(mnt)_2]^{-,3-}$ spectra were taken in the same type of sample tube.

The spectra of the trianion in DME did not show the same degree of motional averaging seen in diglyme. The viscosity, η, of DME at its fp (2.10 cP[23] at ~−70 °C[24,25]) is less than that at −15.5 °C (2.35 cP[18]), the highest temperature for which motionally averaged spectra were taken in diglyme. A spectrum similar to that at −15.5 °C in diglyme was observed at −65 °C in DME; lowering the temperature below −70 °C gave a glassy spectrum less well resolved than that in diglyme at −98 °C. There was no improvement as the temperature was lowered and our analyses did not include the DME spectra.

dx.doi.org/10.1021/jp302598z | J. Phys. Chem. B 2012, 116, 7687−7694

2.3. Glassy ESR Spectrum and *g* Values. Simulation of the trianion's glassy spectrum in diglyme gave $g_x = 2.0824$, $g_y = 2.0660$, and $g_z = 2.2053$ (with relative uncertainties of ± 0.0010); details of their determination, the spectrometer, and other aspects of the ESR methods are given in refs 15 and 16. The assignment of the *g* factors to molecular axes (Figure 1) is by analogy with single crystal results[8] for $[Cu(mnt)_2]^{2-}$, which like $[Ni(mnt)_2]^{3-}$ has a formally d^9 metal ion. The assignment of the largest *g* factor to the out-of-plane *z* direction was confirmed by analysis of the hyperfine splitting of the low field feature in the glassy spectrum of a ^{61}Ni-enriched sample.[7]

Our *g* factors are in reasonable agreement with those in DME (2.081, 2.061, and 2.2055).[6] The largest difference, for g_y, may be due to the reagents used by Geiger et al.[6,7] and ourselves; we both used $(Bu_4N)_2[Ni(mnt)_2]$ but they used a supporting electrolyte with Bu_4N^+ (Bu_4NPF_6) while our reduction produced K^+ ions. All of the trianion's motionally averaged spectra could be simulated using the glassy g_i.[26]

2.4. Calculation of Motionally Averaged Spectra. Freed's theory[27−30] was used for our calculated spectra. Isotropic and axially symmetric reorientation were considered. For the latter, $D_\parallel$ and $D_\perp$ are the diffusion constants for reorientation about the symmetry (parallel) axis and the two perpendicular axes, respectively; $D_\parallel = D_\perp$ for isotropic reorientation. The reorientation was assumed to be taking place via Brownian rotational diffusion (BRD), free diffusion (FD), or jump diffusion (JD), all of which have been used for $[Ni(mnt)_2]^-$,[17] vanadyl complexes,[30] and nitroxides.[27−29] The reorientational correlation times for BRD, FD, and JD are given by[27,28]

$$\tau_L(K)^{-1} = B_L[D_\perp L(L+1) + (D_\parallel - D_\perp)K^2] \quad (1)$$

where $L = 0, 2, 4, \ldots$ and $K = L, L-2, \ldots, -L$. The model-dependent parameter $B_L = [1 + L(L+1)D_\perp\tau]^{-m}$ has $m = 0$, 1/2, and 1 for BRD, FD, and JD, respectively. For FD, a molecule rotates freely for time τ, then reorients instantaneously; for JD, a molecule has a fixed orientation for time τ, then jumps instantaneously to a new orientation.[27] The correlation times $\tau_i = (6D_i)^{-1}$, where $i = \parallel$ and $\perp$, will be used when discussing the monoanion and trianion's motional results.

Spectra were calculated as a function of the magnetic field, *B*, using[27,28]

$$F_0 = (4\pi\beta_e B/3h)[g_Z - (1/2)(g_X + g_Y)] \quad (2a)$$

$$F_2 = [2(6)^{1/2}\pi\beta_e B/3h](g_X - g_Y) \quad (2b)$$

where β_e is the Bohr magneton, *h* is Planck's constant, and the *Z* axis is the rotational diffusion's symmetry axis ($D_\parallel = D_Z$, $D_\perp = D_X = D_Y$). The three possible assignments of the *X*, *Y*, *Z* diffusion axes to the colinear *x*, *y*, *z* magnetic axes (Figure 1) are $D_\parallel = D_x$ ($g_Z = g_x$, $g_X = g_y$, $g_Y = g_z$), $D_\parallel = D_y$ ($g_Z = g_y$, $g_X = g_z$, $g_Y = g_x$), and $D_\parallel = D_z$ ($g_Z = g_z$, $g_X = g_x$, $g_Y = g_y$). All of the monoanion simulations used $D_\parallel = D_y$ and $D_\parallel/D_\perp = 3.0$−4.0;[17] BRD gave agreement with experiment in EtOH and DMF-$CHCl_3$, whereas FD with a small deviation from BRD ($D_\perp\tau = 0.060$) was needed in eugenol, DMPT, TBP, TEHP, and diglyme. The spectra were sensitive to the small change in $D_\perp\tau$ because of the large anisotropy in the monoanion's *g* values.[17] Similarly, the 250 GHz spectra of the nitroxide PD-Tempone[29] were more sensitive to the motional model than those at X-band because of the enhanced *g*-value resolution at the higher frequency. The trianion also has large *g*-value differences and its spectra are sensitive to small changes in $D_\perp\tau$; as is shown below, BRD gives agreement with experiment, whereas FD and JD with $D_\perp\tau = 0.06$ do not.

A typical $[Ni(mnt)_2]^{3-}$ simulation involved a 240 G sweep; the line shape equations were solved in steps of 1 G. The transition moment anisotropy[30] was used as was a rotationally invariant width,[27] T_2^{-1}, in units of F_0; the resulting magnetic field dependence of T_2^{-1} across the 210 G spanned by our glassy *g* values was moderately small, a typical variation being $T_2^{-1} = 7.4$−8.4 G.

3. RESULTS

All of the $[Ni(mnt)_2]^{3-}$ spectra could be simulated using isotropic BRD. The calculated spectra in Figures 3 and 4 show good agreement with experiment for −53.0 and −71.5 °C, respectively; similar agreement was obtained for the other temperatures. As should be the case for isotropic reorientation, identical spectra were obtained regardless of the designation of the diffusional symmetry axis. Those in Figures 3 and 4 were obtained with $D_\parallel = D_x$. A value of $T_2^{-1} = 0.150F_0$ (corresponding to a variation of 7.4−8.4 G across the spectrum) was used for all temperatures except −71.5 and −81 °C where $0.175F_0$ (8.6−9.8 G) was needed. The uncertainty in the values of $D_\perp$ is ±15%; simulations using $D_\parallel = D_x$ and BRD were used to determine limits of 0.75−1.5 for $D_\parallel/D_\perp$.

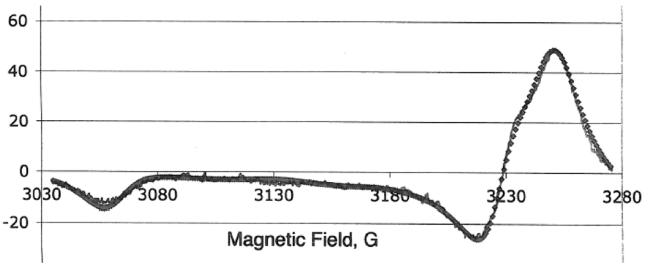

Figure 4. Motionally averaged spectrum of $[Ni(mnt)_2]^{3-}$ in diglyme at −71.5 °C and a spectrum calculated using the glassy g_i, isotropic BRD, $D_\perp = 6.35 \times 10^6$ s^{-1}, and $T_2^{-1} = 0.175F_0$ (8.6−9.8 G).

Figure 5 compares the $[Ni(mnt)_2]^{3-}$ spectrum at −62 °C with one calculated using the motional model employed for $[Ni(mnt)_2]^-$ in diglyme[17] ($D_\parallel = D_y$, $D_\parallel/D_\perp = 3.0$, FD, and $D_\perp\tau = 0.060$). The lack of agreement is obvious and was no better for the other temperatures. Isotropic reorientation with FD and $D_\perp\tau = 0.060$ failed to give agreement with experiment as did simulations calculated for any of the assignments of $D_\parallel$ with

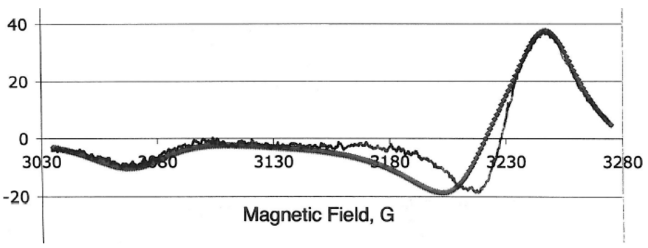

Figure 5. Motionally averaged spectrum of $[Ni(mnt)_2]^{3-}$ in diglyme at −62.0 °C and a spectrum calculated using $D_\perp = 2.5 \times 10^7$ s^{-1}, the glassy g_i, $T_2^{-1} = 0.100F_0$ (7.2−8.2 G), FD with $D_\perp\tau = 0.060$, $D_\parallel = D_y$, and $D_\parallel/D_\perp = 3.0$.

dx.doi.org/10.1021/jp302598z | J. Phys. Chem. B 2012, 116, 7687−7694

values of $D_{\parallel}/D_{\perp} \neq 1$ and either BRD or FD with $D_{\perp}\tau = 0.060$. The lack of agreement with the −62 °C spectrum is seen for $D_{\parallel} = D_z$, $D_{\parallel}/D_{\perp} = 3.0$, and BRD in Figure 6 and for $D_{\parallel} = D_y$,

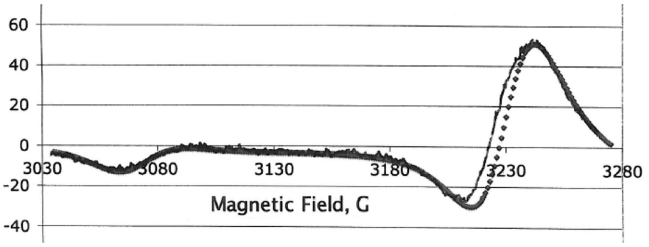

Figure 6. Motionally averaged spectrum of $[Ni(mnt)_2]^{3-}$ in diglyme at −62.0 °C and a spectrum calculated using $D_{\perp} = 2.0 \times 10^7$ s^{-1}, the glassy g_i, $T_2^{-1} = 0.0609F_0$ (7.4−8.4 G), BRD, $D_{\parallel} = D_z$, and $D_{\parallel}/D_{\perp} = 3.0$.

$D_{\parallel}/D_{\perp} = {}^1/_3$, FD, and $D_{\perp}\tau = 0.060$ in Figure 7. Simulations carried out with JD and $D_{\perp}\tau = 0.060$, a larger deviation from BRD than FD and $D_{\perp}\tau = 0.060$, also were unsuccessful.

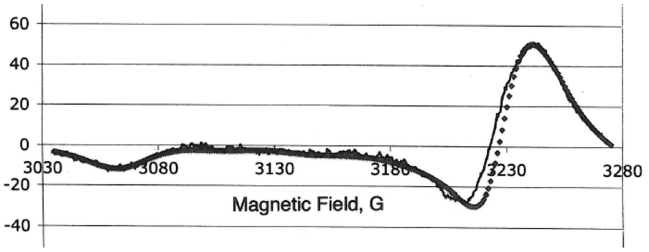

Figure 7. Motionally averaged spectrum of $[Ni(mnt)_2]^{3-}$ in diglyme at −62.0 °C and a spectrum calculated using $D_{\perp} = 4.0 \times 10^7$ s^{-1}, the glassy g_i, $T_2^{-1} = 0.103F_0$ (7.4−8.4 G), FD with $D_{\perp}\tau = 0.060$, $D_{\parallel} = D_y$, and $D_{\parallel}/D_{\perp} = {}^1/_3$.

Figure 8 shows the differences between trianion and monoanion simulations at near-equal temperatures. The

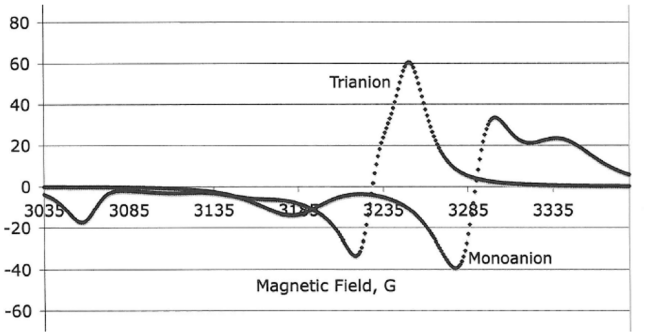

Figure 8. Calculated spectra for $[Ni(mnt)_2]^-$ and $[Ni(mnt)_2]^{3-}$ in diglyme. The monoanion spectrum was calculated using FD with $D_{\perp}\tau = 0.060$, $D_{\parallel} = D_y$, $D_{\parallel}/D_{\perp} = 3.0$, $T_2^{-1} = 0.050F_0$ (1.2−1.4 G), $D_{\perp} = 5.31 \times 10^7$ s^{-1}, $g_X = 1.9954$, $g_Y = 2.1355$, and $g_Z = 2.0426$. The trianion spectrum is the same as that in Figure 4.

trianion's spectrum (at −71.5 °C) has features at ≈3055 and 3235 G, whereas that of the monoanion (at −70.5 °C) has features at ≈3185, 3285, and 3335 G. The simulations are in agreement with the experimental spectra (which are not included).

The motional data obtained from the trianion's spectra are given in Table 1 as are those from our earlier monoanion

Table 1. Motional Parameters and $g_i(T)$ for $[Ni(mnt)_2]^{3-}$ and $[Ni(mnt)_2]^-$ Simulations in Diglyme

ion	T, °C	$10^{-7}D_{\perp}$, s^{-1}	$g_Z(T)$[a]
$[Ni(mnt)_2]^{3-}$[b]	−15.5	20.0	2.0824
	−26.5	16.0	2.0824
	−34.8	12.6	2.0824
	−44.0	9.0	2.0824
	−53.0	4.4	2.0824
	−62.0	2.0	2.0824
	−71.5	0.635	2.0824
	−81.0	0.098	2.0824
$[Ni(mnt)_2]^-$[c]	−65.5	8.0	2.0433
	−70.5	5.3	2.0426
	−73.5	4.0	2.0419
	−76.0	3.1	2.0413
	−78.5	2.5	2.0413
	−84.0	1.2	2.0413
	−88.5	0.59	2.0413

[a]For $[Ni(mnt)_2]^{3-}$, $g_Z(T) = g_x(T)$; for $[Ni(mnt)_2]^-$, $g_Z(T) = g_y(T)$. See ref 26. [b]For isotropic Brownian rotational diffusion ($D_{\parallel}/D_{\perp} = 1.0$); $T_2^{-1} = 0.150F_0$ (which varies from 7.4−8.4 G over the 210 G spanned by the glassy g values) was used except −71.5 and −81.0 °C, for which $T_2^{-1} = 0.175F_0$ (which varies from 8.6−9.8 G) was used. [c]For free diffusion, $D_{\perp}\tau = 0.06$, $D_{\parallel}/D_{\perp} = 3.0$, and $T_2^{-1} = 0.050F_0$ (which varies from 1.2−1.4 G over the 210 G spanned by the glassy g values).

simulations in diglyme.[17,26] Figure 9a shows a plot of these data versus $1/T$, where T is the absolute temperature; included are $\tau_{\perp} = \tau_{\parallel}$ for $[Ni(mnt)_2]^{3-}$ and $\tau_{\perp}$ and $\tau_{\parallel}$ for $[Ni(mnt)_2]^-$. At a common temperature, the values for $[Ni(mnt)_2]^{3-}$ clearly are larger than $\tau_{\perp}$ and $\tau_{\parallel}$ for $[Ni(mnt)_2]^-$. In Figure 9b the results for $[Ni(mnt)_2]^-$ are multiplied by a factor of 9; the values of $\tau_{\perp}$ for the two ions are in approximate agreement although those for the monoanion have a smaller slope. This is consistent with Figure 8, where the temperatures for the two spectra are essentially the same but the monoanion's value of $D_{\perp}$ is larger than that of the trianion by a factor of 8.4.

4. DISCUSSION

4.1. Ion Pairing and Solvent Coordination. The axially symmetric motional model used to simulate the $[Ni(mnt)_2]^-$ spectra[17] suggested a near-prolate-ellipsoidal shape. The isotropic, slower reorientation used for the trianion's simulations implies a more spherical shape and larger size. This is consistent with our earlier work,[16,31] where the translational diffusion constants, D_T, of $[Ni(mnt)_2]^-$ and $[Ni(mnt)_2]^{2-}$ gave different sizes for the two ions. Values of r_t, a length determined by the solute's dimensions[16] were obtained from D_T using the Stokes−Einstein relation ($D_T = k_BT/6\pi\eta r_t$; k_B is Boltzmann's constant). D_T could not be determined for $[Ni(mnt)_2]^{3-}$ because of its air sensitivity.

The values of r_t (with typical uncertainties of ±0.20 Å) are given in Table 2 as are the solvents' dielectric constants, ε_0. The r_t values for $[Ni(mnt)_2]^-$ are essentially the same in acetonitrile (ACN), EtOH, acetone, and BuOH (≈3.60 Å) and are smaller than those for $[Ni(mnt)_2]^{2-}$ in EtOH, acetone, and ACN (≈4.50 Å).[16,31] These results are in agreement with electrochemical,[32] conductivity,[33,34] and vapor phase osmometry[32]

dx.doi.org/10.1021/jp302598z | J. Phys. Chem. B 2012, 116, 7687−7694

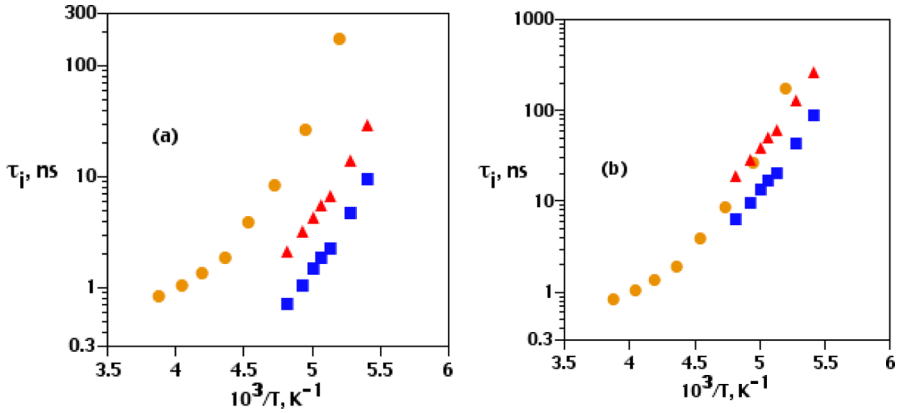

Figure 9. Motional parameters from the simulations for $[Ni(mnt)_2]^{3-}$ and $[Ni(mnt)_2]^{-}$ in diglyme versus $1/T$. Shown in panel a are $\tau_\perp = \tau_\parallel$ for $[Ni(mnt)_2]^{3-}$ (circles), $\tau_\perp$ for $[Ni(mnt)_2]^{-}$ (triangles), and $\tau_\parallel$ for $[Ni(mnt)_2]^{-}$ (squares); the $[Ni(mnt)_2]^{-}$ data are multiplied by a factor of 9 in panel b.

Table 2. Dielectric Constants, Hydrodynamic Radii, and Solute-Solvent Interaction Parameters from the ESR and Translational Diffusion Experiments for $[Ni(mnt)_2]^{-}$ (n = 1) and $[Ni(mnt)_2]^{2-}$ (n = 2)

solvent	ε_0 [a]	$r_t(n=1)$, Å[b]	$r_t(n=2)$, Å[b]	$\kappa_\perp(n=1)$[c]
diglyme	7.65_{25}			0.82
triglyme	7.75_{25}			1.07
tetraglyme	7.70_{25}			0.95
EtOH	24.3_{25}	3.60	4.76	0.85
eugenol	9.7_{20}			0.58
DMPT	8.5_{24}			0.50
BuOH	17.1_{25}	3.44		0.48
TBP	8.1_{25}			0.38
TEHP	$\approx 8.0_{25}$			0.25
ACN	37.45_{20}	3.48	4.20	
acetone	21.3_{25}	3.77	4.54	

[a] From Table 1 of ref 31 except for diglyme from Firman, M.; Xu, M.; Eyring, E. M.; Petrucci, S. *J. Phys. Chem.* **1993**, *97*, 3606–3613. [b] The entries are the averages of the values given in Table 2 of ref 31; typical uncertainties are ±0.20 Å. [c] The entries are from Table 1 from ref 18.

data in ACN that showed $[Ni(mnt)_2]^{2-}$ but not $[Ni(mnt)_2]^{-}$ was ion-paired with Et_4N^+ (we used Bu_4N^+). The absence of ion pairing between $[Ni(mnt)_2]^{-}$ and Bu_4N^+ in diglyme is consistent with infrared studies that indicated a lack of association between Bu_4N^+ and $CF_3SO_3^-$ in both diglyme[35] and triglyme[36] (triethylene glycol dimethyl ether). Solutions of $LiCF_3SO_3$ in the same two solvents, however, contained free ions, contact ion pairs, and aggregates.[35,36]

If the dianion is ion-paired in ACN (ε_0 = 37.45), the trianion should be in diglyme, with its smaller value of ε_0 = 7.65. Both Bu_4N^+ and K^+ are possible pairing partners but the smaller potassium cations with their less shielded charge may be more strongly associated. The glymes are well-known cation solvating media[37] and the K^+ ions also may be coordinated by diglyme. For example, the bis(cyclooctatetraenyl)cerium anion, $[Ce(C_8H_8)_2]^-$, and a diglyme-coordinated potassium cation[38] form a contact ion pair and the bis(*tert*-butyl[8]annulene)ytterbate(II) dianion, $[Yb(C_{12}H_{16})_2]^{2-}$,[39] and 1,3,5,7-tetramethylcyclooctatetraenide, $[C_8H_4(CH_3)_4]^{2-}$,[40] both form trimers with two potassium-diglyme units.

To illustrate the possible changes in shape and size of our paramagnetic species relative to the free trianion, Figure 10 shows two ion-paired arrangements with diglyme-coordinated

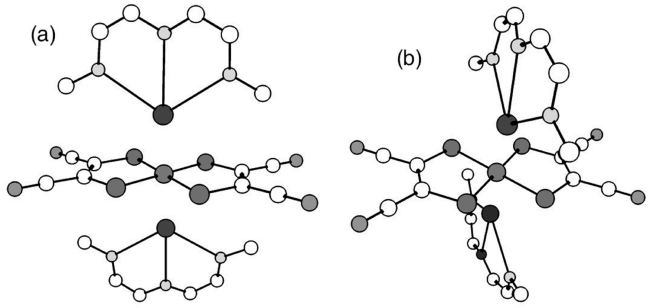

Figure 10. Possible arrangements of diglyme-coordinated potassium ions paired with the trianion. The carbons (open circles) and oxygens (gray circles) of the diglymes are along the y and x axes of the trianion in panels a and b, respectively.

potassium ions. The carbons and oxygens of the diglymes are along the y and x axes of the trianion in Figure 10, panels a and b, respectively. These two preliminary models were prepared using X-ray results for their subunits. Data for the dianion[41] were used for the trianion while the coordinated cations were constructed from the positional and crystal parameters in ref 40. The cations were placed 2.40 Å above the Ni atom by analogy with cation–anion distances in refs 39 and 40. Ion-paired structures with uncoordinated cations are other possibilities with larger volumes and shapes different from that of the free trianion; they as well as the models shown in Figure 10 will be the subjects of electronic structure calculations.

Infrared results also argued against specific solvation of $[Ni(mnt)_2]^{-}$ by ethers. One of the studies[36] of $Bu_4NCF_3SO_3$ showed no significant solvent-anion interaction in triglyme and tetrahydrofuran (THF). Other monoanion-dianion differences and reasons for the absence of monoanion-solvent interactions are discussed in refs 17 and 18.

Gold also has a series of anionic mnt complexes ($[Au(mnt)_2]^{n-}$; n = 1, 2, and 3) whose redox chemistry[42] has been studied in detail. Analyses of cyclic voltammetry scans gave kinetic and equilibrium data that showed the trianion to be associated with both solvent and Bu_4N^+ cations in ACN while it had less solvation and increased ion-pairing in the less polar THF. The diffusion constants of the three gold anions in THF decreased in the order $D_T(1-) > D_T(2-) > D_T(3-)$.[42] This follows the trend for the D_T values of $[Ni(mnt)_2]^{-}$ and $[Ni(mnt)_2]^{2-}$ and the ESR results for $[Ni(mnt)_2]^{-}$ and

dx.doi.org/10.1021/jp302598z | J. Phys. Chem. B 2012, 116, 7687–7694

$[Ni(mnt)_2]^{3-}$. There is, however, a structural difference; the electronic spectrum of the gold trianion suggests it has a tetrahedral or distorted-tetrahedral configuration while the gold monoanion and dianion as well as the three nickel anions are square planar.[42]

4.2. Viscosity-Temperature Dependence of Motional Data. The solute's size also is found in the modified Stokes–Einstein–Debye model[43]

$$\tau_\perp = C_\perp(\eta/T) + \tau_0 \quad (3)$$

where τ_0 is the zero-viscosity intercept, $C_\perp = 4\pi r_0^3 \kappa_\perp / 3k_B$, $\kappa_\perp$ is a radical-solvent interaction parameter, and r_0^3 is a function of r_t and the radical's shape;[44] r_0^3 = 78.0 Å^3 was determined for $[Ni(mnt)_2]^-$.[16] The values of $\kappa_\perp$ for $[Ni(mnt)_2]^-$ (with uncertainties of ±15%)[18] are given in Table 2; they are within the range $(0 \le \kappa_\perp \le 1)$ derived in a theoretical treatment of molecular reorientation.[45,46]

Unfortunately, the values of $\tau_\perp = \tau_\parallel$ for the trianion, although clearly larger than $\tau_\perp$ and $\tau_\parallel$ for the monoanion, are not linear in η/T (Figure 11) and can not be used to obtain a value of $C_\perp$.

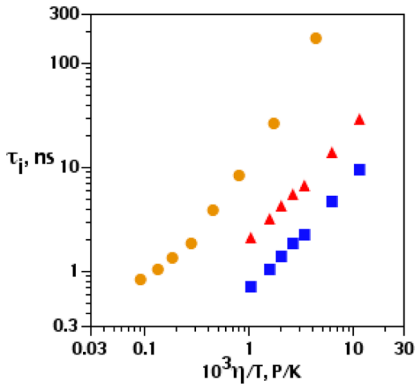

Figure 11. Motional parameters from the simulations for $[Ni(mnt)_2]^{3-}$ and $[Ni(mnt)_2]^-$ in diglyme versus η/T. Shown are $\tau_\perp = \tau_\parallel$ for $[Ni(mnt)_2]^{3-}$ (circles), $\tau_\perp$ for $[Ni(mnt)_2]^-$ (triangles), and $\tau_\parallel$ for $[Ni(mnt)_2]^-$ (squares).

The values of the τ_i for the trianion's four lowest temperatures $(10^3\eta/T \ge 0.46)$ do have a larger slope than $\tau_\perp$ and $\tau_\parallel$ for the monoanion but this is not the case for the four highest temperatures. The nonlinearity in Figure 11 may be due to temperature-dependent changes in the degree of ion pairing and solvent association, both of which can change the size of the paramagnetic probe and its interactions with the solution components.[37,47]

4.3. Spectral Fit Parameters. The values of T_2^{-1} for $[Ni(mnt)_2]^{3-}$ (7.4–8.4 G) are larger than the typical values[17] of 1.2–1.4 G for $[Ni(mnt)_2]^-$ by a factor of ≈6. The increase may be due to inhomogeneous broadening from unresolved hyperfine splittings although it was not necessary to include them in the trianion simulations. Possible sources of such broadening include any ion-paired K^+ or Bu_4N^+ cations, variations in the nature of the ion pairing, protons on coordinated solvent molecules, and the ^{14}N nuclei in the mnt ligands (although their contribution is estimated to be small[48]).

The trianion's spin rotational interaction is somewhat larger than the monoanion's[49,50] but is unlikely to make the dominant contribution to T_2^{-1}. It is expected to decrease with decreasing temperature[30,44] but is constant for the six temperatures between −15.5 and −62.0 °C and then increases for −71.5 and −81.0 °C. The values of T_2^{-1} for the monoanion were independent of temperature in six of the seven solvents for which spectra were simulated; they increased as the temperature decreased in the seventh.[17,51]

The electron transfer (self-exchange) reaction between the dianion and trianion could be a possible source of line broadening if the former was not completely reduced to the latter. The spectra have been simulated without taking this into account but it would not seem to be significant. The values of k_{ex} for the exchange between the monoanion and dianion in acetone and nitromethane at 22 °C were found to be 2.91 × 10^6 and 5.78 × 10^6 M^{-1} s^{-1}, respectively, using ^{13}C NMR.[11] The value of k_{ex} for the dianion-trianion electron exchange would be expected to be smaller, particularly at the lower temperatures the trianion's spectra were taken $(-15.5 \ge T \ge -81.0$ °C). If the concentration of unreduced dianion is 10^{-3} M and $k_{ex} = 6 \times 10^6$ M^{-1} s^{-1} (relatively large values), the trianion's mean lifetime would be $\tau_m = (k_{ex}[\text{dianion}])^{-1} = 1.7 \times 10^{-4}$ s, which is considerably longer than the values of $\tau_2(0) = \tau_\perp$, the reorientational correlation time obtained from the simulations for the second-rank anisotropic Zeeman interaction: 1.7×10^{-7} s (−81 °C) $\ge \tau_2(0) \ge 8.3 \times 10^{-10}$ s (−15.5 °C). Smaller values of k_{ex} and the dianion concentration would give longer values of τ_m.

5. SUMMARY AND CONCLUSIONS

The X-band ESR spectra of the bis(maleonitriledithiolato)-nickel trianion, $[Ni(mnt)_2]^{3-}$, have been taken as a function of temperature in diglyme; it was prepared by reducing $[Ni(mnt)_2]^{2-}$ with potassium metal. The motional model and reorientational rates from simulations of the spectra have been compared with those published previously[17] for the paramagnetic monoanion, $[Ni(mnt)_2]^-$, in the same solvent. The calculated spectra for the trianion used isotropic rotational diffusion, whereas the simulations for the monoanion used axially symmetric reorientation with diffusion about the long in-plane axis three times faster than that about the two perpendicular axes. The reorientation of the trianion was found to be slower than both of the monoanion's reorientational rates. The different motional models and slower reorientation for the trianion suggest that the two ions have different shapes and sizes in solution, with the trianion being larger and more spherical. $[Ni(mnt)_2]^{3-}$ appears to be ion-paired, whereas $[Ni(mnt)_2]^-$, as confirmed by results from other techniques, is not.

■ ASSOCIATED CONTENT

Supporting Information

A detailed description of the procedure followed to reduce $[Ni(mnt)_2]^{2-}$ to $[Ni(mnt)_2]^{3-}$ is given as are all of the motionally averaged experimental spectra of $[Ni(mnt)_2]^{3-}$. This material is available free of charge via the Internet at http://pubs.acs.org.

■ AUTHOR INFORMATION

Corresponding Author

*Phone: 314-977-2837. Fax: 314-977-2521. E-mail: kowertba@slu.edu.

Notes

The authors declare no competing financial interest.

■ ACKNOWLEDGMENTS

The ESR temperature-control unit used in this work was purchased with funds provided by the Beaumont Faculty Development Fund and the Department of Chemistry, St. Louis University. We thank Dr. Chuck Kirkpatrick for his help in preparing Figure 10.

■ REFERENCES

(1) Beswick, C. L.; Schulman, J. M.; Stiefel, E. I. In *Progress in Inorganic Chemistry: Dithiolene Chemistry*; Stiefel, E. I., Ed.; Wiley: New York, 2004; Vol. *52*, pp 55−110.
(2) Geiger, W. E., Jr.; Mines, T. E.; Senftleber, F. C. *Inorg. Chem.* **1975**, *14*, 2141−2147.
(3) Geiger, W. E., Jr.; Barrière, F.; LeSeur, R. J.; Trupia, S. *Inorg. Chem.* **2001**, *40*, 2472−2473.
(4) Gray, H. B.; Williams, R.; Bernal, I.; Billig, R. *J. Am. Chem. Soc.* **1962**, *84*, 3596−3597.
(5) Davison, A.; Edelstein, N.; Holm, R. H.; Maki, A. H. *Inorg. Chem.* **1963**, *2*, 1227−1232.
(6) Mines, T. E.; Geiger, W. E., Jr. *Inorg. Chem.* **1973**, *12*, 1189−1191.
(7) Geiger, W. E., Jr.; Allen, C. S.; Mines, T. E.; Senftleber, F. C. *Inorg. Chem.* **1977**, *16*, 2003−2008.
(8) Maki, A. H.; Edelstein, N.; Davison, A.; Holm, R. H. *J. Am. Chem. Soc.* **1964**, *86*, 4580−4587.
(9) Schmitt, R. D.; Maki, A. H. *J. Am. Chem. Soc.* **1968**, *90*, 2288−2292.
(10) Huyett, J. E.; Choudury, S. B.; Eichorn, D. M.; Bryngelson, P. A.; Maroney, M. J.; Hoffman, B. M. *Inorg. Chem.* **1998**, *37*, 1361−1367.
(11) Kowert, B. A.; Fehr, M. J.; Sheaf, P. J. *Inorg. Chem.* **2008**, *47*, 5696−5701.
(12) Huang, R.; Kivelson, D. *Pure Appl. Chem.* **1972**, *32*, 207−219.
(13) Huang, R.; Kivelson, D. *J. Magn. Reson.* **1974**, *14*, 202−222.
(14) Kowert, B. A.; Broeker, G. K.; Gentemann, S. J.; Fehr, M. J. *J. Magn. Reson.* **1992**, *98*, 362−380.
(15) Kowert, B. A.; Higgins, E. J.; Mariencheck, W. I.; Stemmler, T. L.; Kantorovich, V. *J. Phys. Chem.* **1996**, *100*, 11211−11217.
(16) Kowert, B. A.; Stemmler, T. L.; Fehr, M. J.; Sheaff, P. J.; Gillum, T. J.; Dang, N. C.; Hughes, A. M.; Staggemeier, B. A.; Zavich, D. V. *J. Phys. Chem. B* **1997**, *101*, 8662−8666.
(17) Kowert, B. A.; Broeker, G K.; Gentemann, S. J.; Stemmler, T. L.; Fehr, M. J.; Stemmler, A. J.; Thurman-Keup, E. M.; McCoo, P. W.; Everett, T. B.; Lupo, D. J.; Fitzsimmons, P. K.; Cordero, A. B. *J. Phys. Chem. B* **2007**, *111*, 13404−13409.
(18) Kowert, B. A.; Thurman-Keup, E. M.; Stemmler, A. J.; Stemmler, T. L.; Fehr, M. J.; Caldwell, C. V. C.; Gentemann, S. J. *J. Phys. Chem. B* **2010**, *114*, 2760−2765.
(19) Lipkin, D.; Paul, D. E.; Townsend, J.; Weissman, S. I. *Science* **1953**, *117*, 534−535.
(20) Davison, A.; Holm, R. H. *Inorganic Syntheses*; Muetterties, E. L., Ed.; McGraw-Hill: New York, 1967; Vol. *10*, pp 8−26.
(21) Catterall, R.; Slater, J.; Symons, M. C. R. *J. Chem. Phys.* **1970**, *52*, 1003−1004.
(22) Holton, D. M.; Ellaboudy, A. S.; Edmonds, R. N.; Edwards, P. P. *Proc. R. Soc. London, Ser. A* **1988**, *415*, 121−140.
(23) Carvajal, C.; Tölle, K. J.; Smid, J.; Szwarc., M. *J. Am. Chem. Soc.* **1965**, *87*, 5548−5553.
(24) *CRC Handbook of Chemistry and Physics*, 90th ed.; Lide, D. R., Haynes, W. M., Eds.; CRC Press: Boca Raton, FL, 2009; Sec. 3. *Lange's Handbook of Chemistry*, 15th ed.; Dean, J. A., Ed.; McGraw-Hill: New York, 1999; Table 1.15.
(25) *Merck Index*, 10th ed.; Windholz, M., Budavari, S., Blumetti, R. F., Otterbein, E. S., Eds.; Merck & Co.: Rahway, NJ, 1983. Both handbooks in ref 24 give −69 °C for the fp of DME. Reference 25 gives −71 °C but also lists −58 °C, as do other sources (*2012−14 Handbook of Fine Chemicals*; Sigma-Aldrich Co.: St. Louis, MO, 2011). We tend to favor the lower value because ref 23 reports the densities and viscosities of DME as well as the conductivities of DME−tetraphenylboride salt solutions down to −70 °C.
(26) The $[Ni(mnt)_2]^-$ spectra could be simulated using the glassy values of g_x and g_z but g_y was found to be temperature-dependent with $\Delta g_y/\Delta T > 0$.[17] The values of $g_Z(T) = g_y(T)$ for the monoanion in diglyme are given in Table 1 as are the temperature-independent values of $g_Z(T) = g_x(T)$ for the trianion. The largest difference from the glassy value for the monoanion was $\Delta g_y = 0.0020$ for −65.5 °C. The trianion spectra also are sensitive to the values of the g_i but temperature-dependent values of the g_i were not needed; simulations with values of $\Delta g_i = \pm 0.0020$ did not produce agreement with experiment. More details concerning the $[Ni(mnt)_2]^-$ simulations are given in ref 17.
(27) Freed, J. H. In *Spin Labeling: Theory and Applications*; Berliner, L. J., Ed.; Academic Press: New York, 1976; Vol. *I*, pp 53−132.
(28) Goldman, S. A.; Bruno, G. V.; Polnaszek, C. F.; J. H. Freed, J. H. *J. Chem. Phys.* **1972**, *56*, 716−735.
(29) Borbat, P. P.; Costa-Filho, A. J.; Earle, K. A.; Moscicki, J. K.; Freed, J. H. *Science* **2001**, *291*, 266−269.
(30) Campbell, R. F.; Freed, J. H. *J. Phys. Chem.* **1980**, *84*, 2668−2680.
(31) Kowert, B. A.; Hughes, A. M.; Dang, N. C.; Martin, M. B.; Cheung, G. H.; Tran, H. D.; Reed, J. P. *Chem. Phys.* **1999**, *247*, 435−443.
(32) Lingane, P. J. *Inorg. Chem.* **1970**, *9*, 1162−1166.
(33) Davison, A.; Howe, D. V.; Shawl, E. T. *Inorg. Chem.* **1967**, *6*, 458−463.
(34) Balch, A. L.; Dance, I. G.; Holm, R. H. *J. Am. Chem. Soc.* **1968**, *90*, 1139−1145.
(35) Petrowsky, M.; Frech, R.; Suarez, S. N.; Jayakody, J. R. P.; Greenbaum, S. *J. Phys. Chem. B* **2006**, *110*, 23012−23021.
(36) Frech, R.; Huang, W. *J. Soln. Chem.* **1994**, *23*, 469−481.
(37) Smid, J. In *Ions and Ion Pairs in Organic Reactions*; Szwarc, M., Ed.; Wiley-Interscience: New York, 1972; Vol. *1*, pp 85−151.
(38) Hodgson, K. O.; Raymond, K. N. *Inorg. Chem.* **1972**, *11*, 3030−3035.
(39) Kinsley, S. A.; Streitweiser, A., Jr.; Zalkin, A. *Acta Crystallogr., Sect. B* **1986**, *42*, 1092−1094.
(40) Goldberg, S. Z.; Raymond, K. N.; Harmon, C. A.; Templeton, D. H. *J. Am. Chem. Soc.* **1974**, *96*, 1348−1351.
(41) Kobayashi, A.; Sasaki, Y. *Bull. Chem. Soc. Jpn.* **1977**, *50*, 2650−2656 . Figures 10a and 10b were prepared using Chemcraft Version 1.6 (www.Chemcraftprog.com).
(42) LeSuer, R. J.; Geiger, W. E., Jr. *Inorg. Chem.* **2009**, *48*, 10826−10836.
(43) Evans, G. T.; Kivelson, D. *J. Chem. Phys.* **1986**, *84*, 385−390.
(44) Hwang, J.; Kivelson, D.; Plachy, W. *J. Chem. Phys.* **1973**, *58*, 1753−1765.
(45) Kivelson, D.; Kivelson, M. G.; Oppenheim, I. *J. Chem. Phys.* **1970**, *52*, 1810−1821.
(46) The values of $C_\perp$ (and $\kappa_\perp$) for $[Ni(mnt)_2]^-$ in diglyme were obtained from an analysis of the monoanion's principal line widths,[18] which was carried out over a wider range of motional rates than the simulations. The values of $D_\perp$ obtained from the simulations were in reasonable agreement with those from the width analysis.[17,18]
(47) Szwarc, M. In *Ions and Ion Pairs in Organic Reactions*; Szwarc, M., Ed.; Wiley-Interscience: New York, 1972; Vol. *1*, pp 1−26.
(48) Maroney and co-workers[10] used isotopomers of $[Ni(mnt)_2]^-$ and ^{15}N ENDOR to determine the principal values of the nitrogens' hyperfine tensor; they give a ^{14}N isotropic hyperfine splitting constant $a_{iso} = 0.14$ G. We calculated the ESR line shape for four equivalent ^{14}N nuclei using this value of a_{iso} and a peak-to-peak width of 5.68 G for each of the nine Lorentzian hyperfine lines. The unresolved singlet had a peak-to-peak width of 5.72 G, a difference of less than 1% from the intrinsic width. Note that 5.68 G is less than the typical values of T_2^{-1} = 7.4−8.4 G used for the trianion simulations and that a_{iso} for the trianion's ^{14}N nuclei is probably smaller than 0.14 G. Analysis of the g factors[6] and ^{61}Ni hyperfine interaction for the trianion[7] indicated that

the unpaired electron was more highly localized on Ni than in the monoanion, with rather little in-plane covalency.[7]

(49) The spin rotational interaction's peak−peak width in the fast motional limit is given by[12,50] $\Delta B_{SR} = \{2/[9(3)^{1/2}\gamma]\}\sum_i (g_i - g_e)^2/\tau_i$, where γ is the electronic magnetogyric ratio, g_e is the free electron g factor, and τ_i is the reorientational correlation time about the ith molecular axis. If isotropic BRD is used for $[Ni(mnt)_2]^{3-}$ and FD with $D_\perp\tau = 0.060$, $D_\parallel = D_y$, and $D_\parallel/D_\perp = 3.0$ are used for $[Ni(mnt)_2]^-$, one has $\Delta B_{SR}(\text{trianion})/\Delta B_{SR}(\text{monoanion}) = 2.70$ for the same $D_\perp$. This does predict a larger nonreorientational width for the trianion but (a) a value of 2.70 is more than a factor of 2 smaller than the ratio of ≈6 obtained from the simulation parameters, (b) our $[Ni(mnt)_2]^{3-}$ spectra are not in the fast motional limit, and (c) the values of T_2^{-1} show the wrong temperature dependence for a spin rotational contribution.

(50) Zager, S. A.; Freed, J. H. *J. Chem. Phys.* **1982**, *77*, 3344−3359.

(51) Only in EtOH was T_2^{-1} temperature dependent; the variation across the spectrum was 0.6−0.7 G for four temperatures in the range $-88 \geq T \geq -104$ °C and 1.2−1.4 G for three spectra between −111 and −125 °C. The temperature-independent variation was 1.2−1.4 G in the other solvents.